First Principles Hartree-Fock Cluster Study Of Very Dilute Transition Metal And Rare-Earth Ion Systems In Silicon

R.H. Pink[a], S.R. Badu[a], A. Dubey[b], R.H. Scheicher[c], J. Jeong[a], S.R. Byahut[d], L. Chow[b], M.B. Huang[a], and T.P. Das[a,b]

[a]*State University of New York at Albany*
1400 Washington Ave. Albany, New York, 12222.
[b]*University of Central Florida*
4000 Central Florida Blvd., Orlando, Florida 32816.
[c]*Uppsala University*
Uppsala, Sweden
[d]*Tribhuvan University*
Kathmandu, Nepal

Abstract. The locations and electronic structures of dilute Mn^{2+} and Er^{3+} impurity ions in silicon are studied using the Hartree-Fock Cluster procedure including relaxation in the positions of neighbors of the impurity ions. Three likely sites are studied, hexagonal intersititial (H_i), tetrahedral interstitial (T_i) and substitutional (S). Of these, H_i is found to be unstable and S has larger binding energy than T_i, the latter being found to be the occupied site by channeling measurements. This is also supported by the agreement between our theoretical result and experiment for the Mn^{2+} ion magnetic hyperfine constant. A possible reason for the observation of the T_i site experimentally is suggested.

Keywords: Silicon, Magnetic Hyperfine, Hartree-Fock, Hexagonal Interstitial, Tetrahedral Interstitial, Substitutional.
PACS: 71.15.-m

INTRODUCTION

There is currently great interest in the doping of silicon with transition metal and rare-earth ions for studying magnetic properties for the former and optoelectronic and optical transmission applications in the latter. Mn^{2+} ion (used to dope silicon), has been shown to produce ferromagnetism[1] at room temperature with potential applications for spintronics[2]. As far as the rare-earth ion Er^{3+} is concerned, when it is used to dope silicon, it leads to photoluminescence[3] with 1.54 μm wavelength, especially strong in the presence of co-dopants[4] like carbon, nitrogen, oxygen, and fluorine. This photoluminescence involves a very weak frequency dependence on the environment and corresponds to the minimal optical loss in quartz fibers[5]. This makes the Er^{3+}-Si system an attractive candidate for optoelectronic applications such as communication between silicon chips through light, and important improvement in light transmission in fiber optics. For the understanding of ferromagnetism for transition metal-semiconductor systems, a knowledge of the nature of the exchange

CP1003, *Magnetic Materials, International Conference on Magnetic Materials (ICMM-2007)*
edited by A. Ghoshray and B. Bandyopadhyay

interaction between transition metal impurity ions in semiconductors would be very helpful. The exchange interaction between impurity ions is expected to depend on their locations and their electronic wave-functions and the associated spin distributions. Before attempting to understand the use of first-principles[6] Hartree-Fock procedure combined with study of many-body effects by many-body perturbation theory procedure[7] to study non-dilute impurity systems, it is important to test them for very dilute impurity systems. The results of theoretical investigation of very dilute systems are important because there are magnetic hyperfine interaction data available[8,9] for very low concentrations of impurity ions in silicon, where they can be considered as isolated impurities, to test the accuracy of the calculated spin distributions in these systems. For the rare-earth-silicon systems, the main focus for understanding their electronic structures is on the dilute systems which are the pertinent ones for optoelectronic and optical transmission applications.

The present work will deal with the locations of Mn^{2+} and Er^{3+} in silicon with very low concentrations using Hartree-Fock procedure[7] for investigating the electronic structure. The Mn^{2+} and Er^{3+} locations will be compared with results from channeling measurements by our experimental group. Electronic wave-functions obtained from our investigations will be used to study the ^{55}Mn hyperfine interactions constant which will be compared with experiment[8, 9] including estimates of relativistic and many body effects based on results on Mn^0 atom from relativistic many body theory[7]. For Er^{3+}-Si system no hyperfine data are currently available from EPR measurements[10], but one can expect in the future for ^{166}Er and ^{167}Er from Mossbauer[11] and ENDOR measurements[12].

PROCEDURE

The procedure we are using for our investigations of the very dilute Mn^{2+} and Er^{3+} impurity system in silicon including their locations[13] is the Unrestricted Hartree-Fock (UHF) Cluster procedure. It uses a cluster with a finite number of atoms or ions (or molecules for molecular solids) with the same symmetry as the solid state system to simulate the latter, and has been used by our group for a wide variety of systems[14]. The UHF procedure, involving different spatial characters of the electronic wave-functions for up and down spin states in magnetic systems, is necessary to use for studying magnetic hyperfine interactions, in order to include exchange polarization effects of the paired spin states.

The UHF Cluster procedure is first principles in nature for electronic structure investigations. It is well suited to include many-body effects in a quantitative manner because the Hartree-Fock procedures have strictly no many-electron correlation effects and the latter can be introduced accurately and unambiguously by many-body perturbation theory[7], known to be accurate up to 1-2% for many properties of atomic systems[15]. Also it is well suited for hyperfine interactions studies because it uses first principles Hartree-Fock formalism for exchange and so the rapid variation of the electron density and the potential near the nucleus is not a significant problem as it can be[16] in the density-functional approximation for exchange interactions. The main limitation of the Hartree-Fock Cluster procedures is that it does not deal explicitly with the infinite solid, so that convergence[6] with respect to cluster size needs to be tested to

consider the method as representative of the infinite system. This feature is handled carefully in the present investigation and in all our earlier studies in other condensed matter systems[14].

The UHF cluster procedure and its use in obtaining the magnetic hyperfine parameters A and B in the spin-Hamiltonian[18] are described in the literature including Ref. 6. We shall quote the appropriate expressions in terms of the one-electron wave-functions from the UHF procedure. First we shall give the expression for the binding energy (B.E.) for the three sites H_i, T_i, S of the impurity ion shown in Fig. 1, namely,

$$\text{B.E.} = E_{\text{silicon cluster without impurity}} + E_{\text{free impurity ion}} - E_{\text{cluster with impurity}} \tag{1}$$

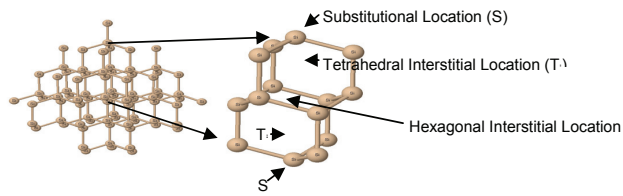

FIGURE 1. Possible lattice locations of the doped ion in silicon.

A positive value of the B.E. for a site indicates that it represents a stable position for the magnetic impurity while a negative value of B.E. suggests that the site is unstable. As will be discussed in detail in Section III dealing with our results, the binding energies of the tetrahedral interstitial and substitutional sites T_i and S respectively after taking account of relaxations up to the second nearest silicon neighbor were positive, and also the total energies of the clusters containing the Mn^{2+} impurity ion had minima at these sites, so they were stable. The hexagonal interstitial H_i site however had a maximum in the total energy of the cluster containing it and so was unstable.

The spin Hamiltonian[18] for magnetic hyperfine tensor for axial symmetry has the form

$$H'_{Spin} = A(\vec{I}\cdot\vec{S}) + B(2I_zS_z - I_xS_x - I_yS_y) \tag{2}$$

The value of A obtained in the above way is given by[6]

$$A = A_{\text{direct}} + A_{EP} \tag{3}$$

$$A_{\text{direct}} = \frac{2\gamma_e\gamma_N\hbar^2}{3S}\sum_i |\psi_{ui}(0)|^2 \tag{4}$$

$$A_{EP} = \frac{2\gamma_e\gamma_N\hbar^2}{3S}\sum_i \left[|\psi_{p\uparrow i}(0)|^2 - |\psi_{p\downarrow i}(0)|^2 \right] \tag{5}$$

Because H_i which has axial symmetry, is not a stable site and T_i and S have tetrahedral symmetry with B=0, so A is the only term that we have to evaluate.

In Eqs. (4) and (5), the summation in i is over all the occupied one-electron states of the cluster. A_{direct} refers to the direct contributions from the electrons in the unpaired spin states with wave-functions ψ_{ui} and the contribution A_{EP} refers to the exchange polarization terms[6] arising from the paired spin states including the core electrons of the impurity ion or silicon atoms for their respective hyperfine properties.

Many-electron correlation effects are rather difficult to introduce directly in the impurity ion-silicon system because of the large number of atoms and basis state orbitals involved in our work. For the hyperfine interaction for the ^{55}Mn nuclei we have estimated in Section III the influence of many-electron correlation effects[15] using the results of accurate investigations of free Mn^0 atom[19] by the many-body perturbation theoretical procedure. The nuclear magnetic moment used for ^{55}Mn in our work is 3.4687190(9) taken from tabulated values in the literature[20].

RESULTS AND DISCUSSION

Figs. 2(a-c) show the clusters used for the H_i, T_i and S positions of the Mn^{2+} ion and the silicon atoms up to the second nearest neighbors of Mn^{2+}. The second nearest silicon neighbors have their dangling bonds terminated by hydrogen atoms. With these choices, the clusters for the three sites are designated as $Mn^{2+}Si_{18}\ H_{36}$ (H_i), $Mn^{2+}Si_{14}\ H_{24}$ (T_i) and $Mn^{2+}Si_{16}H_{36}$(S) clusters.

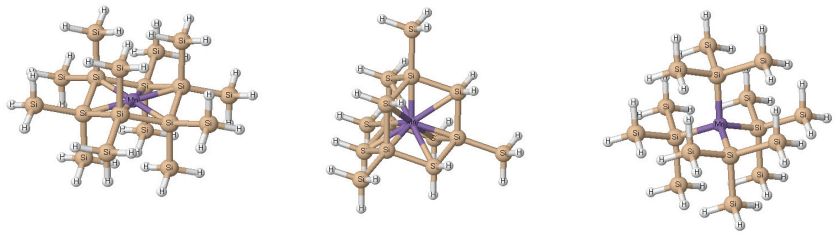

(a) H_i 2NN Cluster (b) T_i 2NN Cluster (c) S 2NN

FIGURE 2. (a) Hexagonal Interstitial 2NN Cluster including upto second nearest neighbor silicons. (b) Tetrahedral Interstitial 2NN Cluster (c) Substitutional 2NN Cluster, for Mn^{2+} impurity systems.

TABLE 1. Energies (in Hartrees) and B.E. (Hartrees and eV) Mn^{2+} impurity in silicon for H_i, T_i, and S sites including first and second nearest neighbors without relaxation.

	H_i 631g(d,p)	H_i 6311g(d,p)	T_i 631g(d,p)	T_i 6311g(d,p)	S 631g(d,p)	S 6311g(d,p)
$Mn^{+2}Si_xH_y$ [a]	-6370.41000	-6370.82195	-5207.96069	-5208.29226	-5792.01800	-5792.37175
Si_xH_y [a]	-5221.40640	-5221.75873	-4058.89971	-4059.17233	-4643.07564	-4643.39515
Mn^{2+}	-1148.96839	-1149.03632	-1148.96839	-1149.03632	-1148.96839	-1149.03632
BE	0.03521	0.02689	0.09260	0.08360	-0.02603	-0.05973
BE (eV)	0.95823	0.73172	2.51976	2.27487	-0.70821	-1.62522
a. x=18, y=36 for Hi; x=14, y=24 for Ti; x=16, y=36 for S						

Table 1 shows the total energies (in Hartree units) in Fig. 2 of these clusters, of the clusters with Mn^{2+} absent, and the total energy of the free Mn^{2+} ion, the three sets of total energies needed in Eq.(6) for the binding energies (B.E.) of the Mn^{2+} ion at the three sites. These B.E. are given in both Hartree units and eV. The total energies and

B.E. are given for two sizable choices[17] of basis sets 6-31g (d,p) and 6-311g (d,p), the (d,p) indicating that extra single d and p Gaussian functions are added[17] to give more flexibility for the s, p, d functions to the 6-31g and 6-311g basis sets to include polarization effects in the Mn^{2+} ion and neighboring Si atoms.

The results in Table 1 show that there is good convergence in the total energies of the clusters with the two basis sets and reasonable convergence for the B.E. for the H_i and T_i sites and somewhat weaker convergence for the S site. Although the H_i site shows positive binding energy it is considered unstable because as mentioned in Section II, it has a maximum in the total energy in the <111> direction. We therefore did not carry out a study of relaxation effects for the H_i site.

Table 2 presents the results of our calculation of the influence of relaxations in positions of the first and second nearest neighbors (1NN and 2NN) of $Mn^{2+}Si_{14}H_{24}$ and $Mn^{2+}Si_{16}H_{36}$ clusters respectively for the T_i and S sites with the 6-311g(d,p) choice of basis sets. Also included in this Table are the $Si_{14}H_{24}$ and $Si_{16}H_{36}$ clusters in the absence of Mn^{2+} as in Table 1 as well as free Mn^{2+} and the corresponding B.E. in Hartree units and eV. We would like to briefly mention here the procedure used for our study of the relaxation of the nearest and second nearest neighbors of Mn^{2+}. This was done iteratively, with total energy optimization, for the two sets of neighbors, first relaxing the 1NN Si, keeping the 2NN Si fixed to get the minimum energy. Next the 1NN Si were fixed at their relaxed positions and the 2NN Si were relaxed and the iterative process involving the two steps was repeated one more time. Throughout the iterative study of the relaxations in positions of the 1NN Si and 2NN Si, the terminal H atoms simulating the influence of the Si atoms outside the cluster were kept fixed.

TABLE 2. Energies (in Hartrees) and B.E. (Hartrees and eV) of Mn^{2+} Impurity in Silicon for T_i and S sites including Relaxation of 1NN and 2NN Silicons indicated in the first line for both Ti and S.

Binding Energies Including Relaxation					
T_i	**0.0Å; 0.0Å**	**0.10Å; 0.0Å**	**0.10Å; 0.06Å**	**0.12Å; 0.06Å**	**0.12Å; 0.07Å**
$Mn^{+2}Si_{14}H_{24}$	-5208.29226	-5208.33568	-5208.33716	-5208.33879	-5208.33957
$Si_{14}H_{24}$	-4059.17233	-4059.17236	-4059.17236	-4059.17236	-4059.17236
Mn^{2+}	-1149.03632	-1149.03635	-1149.03635	-1149.03635	-1149.03635
BE	0.08360	0.12697	0.12845	0.13008	0.13086
BE (eV)	2.27487	3.45493	3.49523	3.53965	3.56088
S	**0.0Å; 0.0Å**	**0.27Å; 0.0Å**	**0.27Å; 0.07Å**	**0.32Å; 0.07Å**	**0.32Å; 0.08Å**
$Mn^{+2}Si_{16}H_{36}$	-5792.37175	-5792.64790	-5792.67944	-5792.68074	-5792.68138
$Si_{16}H_{36}$	-4643.39515	-4643.39516	-4643.39516	-4643.39516	-4643.39516
Mn^{2+}	-1149.03632	-1149.03635	-1149.03635	-1149.03635	-1149.03635
BE	-0.05973	0.21638	0.24792	0.24922	0.24987
BE (eV)	-1.62522	5.88807	6.74635	6.78178	6.79923

From Table 2, as far as the 1NN and 2NN silicon relaxations are concerned, the converged total energies at the fourth iterative steps of energy minimization show very well conserved total energies for the T_i and S clusters. The B.E. for the third and fourth iterative steps, from Table 2, shows good convergence, namely about 6% and 2.5% respectively for T_i and S sites. Comparison of the B.E. with the results from the third columns of Table 2, with only the nearest neighbors relaxed, indicate that the relaxations of the second nearest neighbors lead to increases in B.E. of only about 3% and 15% respectively for the T_i and S sites over those due to the relaxation of the first

neighbors alone. These results suggest that the effects of third nearest neighbor relaxation would not be expected to make significant changes to the B.E. for the T_i and S sites of Mn^{2+} from the values obtained with converged 1NN and 2NN relaxations.

Our results for the B.E. for the T_i and S sites with the latter about twice as large as for T_i, suggest that the S site is more stable than the T_i site and that Mn^{2+} would be expected to be found there most abundantly in dilute Mn-Si system. Recent channeling experiments from our group[21], however suggest that the T_i site is the occupied site, while the S site cannot be ruled out. The resolution of this difference between channeling measurements and our expectations based on B.E. considerations can perhaps be resolved by the following argument. This is that the probability of formation of the S site on Mn^{2+} ion implantation is smaller than for the T_i site. The latter site arises from the trapping of Mn^{2+} at an empty interstitial site in pure silicon. A trapping of Mn^{2+} at the S site on the other hand would require the knocking out of a Si atom to make room for the Mn^{2+} ion during the implantation process or the existence of a Si vacancy already present which can be occupied by the Mn^{2+} ion. Both these possibilities make the formation of a trapped Mn^{2+} S site less likely than the T_i site.

Er^{3+}-Si System Sites for Location of Er^{3+} Ion

For the Er^{3+}-Si system which is very important for optoelectronic-systems and optical transmission, we have also studied the possible location of Er^{3+} ion for H_i, T_i, and S sites as in the case of the Mn^{2+} ion. One main difference in the procedure was that because of the large number of electrons and electronic states in Er^{3+}, we had to use a pseudopotential treatment[17] for the silicon atoms for larger clusters, with the 1s, 2s, and 2p core states kept frozen, not taking part explicitly in the Er^{3+}-Si and Si-Si interactions, only 3s and 3p states being used for the Si atoms in the cluster. As will be seen for the B.E. results for the Er^{3+} ion in silicon at the H_i, T_i, and S sites in Table 3 to be discussed later, we have studied the B.E. for Er^{3+} ion at the T_i site using a cluster involving the 1NN and 2NN silicon neighbors using both all-electron and pseudopotential procedures, and find good agreement between them.

Two other minor differences in the procedure used for the Er^{3+}-Si system as compared to the Mn^{2+}-Si system are the following. One of these is in the process of studying relaxation of the 1NN and 2NN silicons of Er^{3+} through energy minimization. Instead of the stepwise study of 1NN and 2NN silicon relaxation through energy optimization for Mn^{2+}-Si discussed before, a somewhat different procedure was employed for the Er^{3+}-Si system. The total energies of the Er^{3+} clusters were studied as a function of 1NN displacements, with the 2NN displacement determined for each set of positions of the 1NN by energy optimization, and from these studies the minimum total cluster energies and the associated 1NN and 2NN relaxations were obtained. The other difference in the procedure is in the choice of the sizes of the clusters for the Er^{3+}-Si clusters, the second nearest neighbors (2NN) (and third and fourth nearest silicon neighbors (3NN) and (4NN) where these are used) being chosen based on the distances from the Er^{3+} ion, instead of as the nearest neighbors of the 1NN. These two differences in procedure are not expected to have significant influence on the B.E. of the H_i, T_i, and S sites.

Table 3. B.E. (eV) of the Er^{3+} ion in clusters including relaxations of 1NN and 2NN Si.

Cluster (H_i)	**$Er^{3+}Si_{14}H_{20}$**		
Relaxation	1NN=0.0Å 2NN=0.0Å	1NN=0.10Å 2NN=0.0Å	1NN=0.10Å 2NN=0.05Å
B.E.(PP)	-13.3294	-7.3832	-7.2999
Cluster (T_i)	**$Er^{3+}Si_{10}H_{16}$**		
Relaxation	1NN=0.0Å 2NN=0.0Å	1NN=0.12Å 2NN=0.0Å	1NN=0.12Å 2NN=0.10Å
B.E.(PP)	-7.6757	-5.0438	-4.2369
B.E. (All El.)	-7.2305	-4.7707	-4.0663
Cluster (Ti)[a]	**$Er^{3+}Si_{26}H_{48}$**		
Relaxation	1NN=0.0Å 2NN=0.0Å	1NN=0.20Å 2NN=0.0Å	1NN=0.20Å 2NN=0.12Å
B.E.(PP)	-2.8578	0.3014	1.405
Cluster (S)	**$Er^{3+}Si_{16}H_{36}$**		
Relaxation	1NN=0.0Å 2NN=0.0Å	1NN=0.60Å 2NN=0.0Å	1NN=0.60Å 2NN=0.07Å
BE(PP)	-1.1454	4.7092	5.6274

a. Larger Cluster containing Er^{3+} ion and up to Fourth Nearest Neighbor (4NN) Si but with only 1NN and 2NN Si Relaxed.

The B.E. and the relaxations in Si atom positions for H_i, T_i, and S sites for Er^{3+} ions shown in Table 3 have the following features. First the B.E. for different sites were in general very sensitive to the sizes of the clusters chosen for them and to the relaxations in the positions of the 1NN and 2NN Si, features similar to those found for Mn^{2+}-Si.

The B.E. for the H_i site for Er^{3+} with 1NN and 2NN Si included in the cluster were found to be negative for both the cases of no relaxation, and 1NN and 2NN relaxation, in contrast to the Mn^{2+}-Si case where they were positive. For this reason, as well as the fact that the total cluster energy for the H_i site was also a maximum, we were again led to the conclusion that this site was unstable for the location of Er^{3+} ion.

For the T_i site, in contrast to the case of Mn^{2+}-Si system, the B.E. of Er^{3+} was negative without and with relaxation of the 1NN and 2NN silicon neighbors using the cluster including silicons up to the 2NN. For this choice of the T_i cluster, as may be seen from Table 3, the B.E. although negative, were quite close to each other for both the pseudopotential and all electron treatments, providing support for the values of the B.E. for Er^{3+} found for the rest of the clusters, using the pseudopotential procedure, including the results for the cluster for the H_i site just discussed.

On expanding the T_i cluster to the larger one, $Er^{3+}Si_{26}H_{48,}$ including the third and fourth nearest Si neighbors of Er^{3+} without any relaxation, the B.E. without relaxation was again found to be negative but smaller in magnitude then for the smaller T_i cluster indicating an important improvement for the larger cluster. On allowing for the relaxation of 1NN and 2NN Si, the B.E. was found to be positive showing stability of Er^{3+} at the T_i site.

For the S site as can be seen from Table 3, using the cluster involving the 1NN and 2NN Si without any relaxation, the B.E. was negative but smaller in magnitude, about 40% of that for the smaller T_i cluster. On including lattice relaxation involving the 1NN and 2NN Si, the B.E. was found to be positive and nearly four times that for the larger cluster at the T_i site. The relaxations of the 1NN and 2NN Si for the T_i and S sites show the same trend of larger 1NN relaxation for the S site as found for the Mn^{2+} case. However the ratio of the 1NN displacements for the S site for the Er^{3+} case is a

factor of three larger compared to the T_i site in contrast to a factor of two for the case of Mn^{2+}, not unexpected because the Er^{3+} is a larger ion than Mn^{2+}.

Our result of greater binding energy for the S site for Er^{3+} as compared to the T_i site is in agreement with that from a recent investigation[13] by a very different procedure. It used the supercell band structure procedure[22] and used the local density functional approximation for exchange. This agreement in the trend between the results for S and T_i sites using two very different procedures increases the confidence in the correctness of the greater binding energy for the S site that we have found as compared to T_i.

Lastly as in the case of Mn^{2+} in silicon, the most recent results[23] from channeling measurements for Er^{3+}-Si system suggest that the Er^{3+} ion is observed at the T_i site. One can apply the same reasoning for the Mn^{2+}-Si system regarding the relative openness of the T_i site as compared to the S site, leading to greater formation probability for the T_i site as compared to the S site, to explain the channeling results even though the S site is found from Table 3 to have B.E. higher than the T_i site.

Magnetic Hyperfine Interactions

From our UHF calculation we have obtained the relaxed positions of the 1NN and 2NN Si for the Er^{3+} sites in Table 2 and B.E of Er^{3+} for these sites. Our calculation gives as byproducts the electronic wave-functions for the occupied one electron sites. Using these wave-functions we have calculated the Fermi contact contributions given by Eqs.(3-5), in the Procedure Section for the Mn^{2+} ion. The value of the magnetic moment of ^{55}Mn used[20] is 3.4687190(9) nuclear magnetons (μ_N). The values of A including the direct and exchange polarization contributions for the two sites for Mn^{2+} are found to be:

$$A(T_i) = -262.5 \text{ MHz} \quad (6)$$
$$A(S) = -147.0 \text{ MHz} \quad (7)$$

.

The values for $A(T_i)$ and A(S) in Eqs. (6-7) refer strictly to results of non-relativistic one electron theory used in our work, so they do not include any many-body or relativistic effects at all. Fortunately, there are results available from accurate relativistic and non-relativistic diagrammatic many-body perturbation theory investigations[7] on $^{55}Mn^0$ atom. The results of first-principles Dirac Hartre-Fock theory combined with many-body perturbation theory for many-electron contributions to the hyperfine constant A for $^{55}Mn^0$ atom leads to -72.422 MHz in excellent agreement (better than 2.5%) with the experimental value[24] of -74.1 MHz.

A comparison of the non-relativistic and relativistic results[19] for the one-electron and many-electron contributions from the first-principles investigation on Mn^0 atom, leads to about +8.6% and +21.1% for relativistic corrections and many-electron effects respectively for the hyperfine constant A. The net total of +29.7% represents the combined effects of many-body and relativistic corrections to the non-relativistic UHF contribution for the Mn^0 atom. Taking this as an estimate of the net percentage effect of many-body and relativistic corrections to our one-electron contributions to the isotropic hyperfine constants in Eq (6) and Eq (7) the net hyperfine constants $A_{total}(T_i)$ and $A_{total}(S)$ are obtained as:

$$A_{total}(T_i) = -182.5 \pm 13.7 \text{ MHz} \quad (8)$$
$$A_{total}(S) = -102.0 \pm 7.7 \text{ MHz}. \quad (9)$$

The confidence limits in Eqs. (8-9) are obtained allowing for an uncertainty of as much as 25% in the estimated total correction for relativistic and many-body effects because they were obtained from atomic Mn^0 investigations and not in solid state. The experimentally measured[9] value of A in Mn^{2+}-Si is -160.5 MHz which clearly supports the theoretical result for the T_i site in Eq. (8) over the S site result in Eq. (9). We have also included the influence of adding diffuse functions[17] to the (6-311g) basis set for our Mn^{2+}-Si investigation, on the hyperfine constant for the Mn^{2+}-Si system. This leads to a reduction of the magnitude of the theoretical result, yielding $A_{total}(T_i)$ of (-176.6 ± 13.7) MHz, further improving the agreement between theory and experiment.

Thus the ^{55}Mn EPR data also support the presence of the Mn^{2+} ion at the T_i site as found experimentally from channeling data[21] from our group. This EPR data also lends support to the explanation proposed earlier in this Section for the occurrence of Mn^{2+} at the T_i site rather than S which has higher binding energy, namely the possibility that the T_i site has greater probability for formation than the S site.

We have not discussed the ^{29}Si hyperfine interactions of the Silicon neighbors in Mn^{2+}-Si which can be obtained from our wave-functions for the T_i and S sites because we are not aware of any experimental data for ^{29}Si from ENDOR measurements. It is hoped that such data will be available in the future to compare with theoretical predictions for T_i and S sites and provide further information about the correctness of the assignment of Mn^{2+} to the T_i site.

There are no experimental measurements available for the hyperfine interaction constants for Er nuclei. Also one could in principle obtain the non-relativistic one-electron contribution to the isotropic hyperfine interaction constant A(^{166}Er) from our calculated electronic wave-functions for the Er-Si system as in the case of Mn^{2+} ion in silicon. However, accurate first-principle relativistic many-body investigations of hyperfine interactions on rare-earth atomic systems[25,26] like Eu^0 and Gd^{3+} ion have shown that unlike the transition metal ions such as Mn^{2+}, the influences of relativistic and many-body effects are much stronger and that there are also strong cancellations between the contributions from exchange polarization contributions to the hyperfine constants from different shells. This makes the estimation of relativistic and many-body corrections to results from non-relativistic Hartree-Fock investigations more difficult for Er^{3+} than for Mn^{2+}. Nevertheless estimation of such corrections should be attempted in the future when experimental results for hyperfine interactions are available for instance from Mössbauer measurements in ^{153}Er nucleus. Also as in the case of the Mn^{2+}-Si system, it would be interesting to have experimental ^{29}Si hyperfine interaction constants from ENDOR measurements[12] to compare with theoretical predictions using our calculated electronic wave-functions for the Er^{3+}-Si system.

CONCLUSIONS

Using the Hartree-Fock cluster procedure, we have investigated the binding energies and locations of Mn^{2+} and Er^{3+} ions, including the relaxations in positions of

the silicon neighbors. The results are sensitive to relaxation effects, with sizable relaxation of the nearest neighbors and smaller but significant relaxation of the second nearest ones. For both the ions, the hexagonal interstitial position is unstable having a maximum in the energies of the associated clusters for both ions. The T_i and S sites have energy minima and positive binding energies indicating stability, with the binding energy for the S site significantly larger than for the T_i. However recent channeling measurements[21, 23] suggest that T_i is the occupied site although S cannot be ruled out. For Mn^{2+} ion, our calculated isotropic Fermi contact hyperfine constant for the T_i site is in satisfactory agreement with the results from electron paramagnetic resonance experiments[9], providing further support to the T_i position for Mn^{2+} in silicon. A possible reason for this situation is suggested. Success of the UHF procedure in explaining the observed T_i location of the Mn^{2+} ion and its hyperfine constant, including many-body contributions for the latter, suggests that a similar procedure would be helpful for understanding the ferromagnetic Mn^{2+}-Si system.

REFERENCES

1. M. Bolduc, C. Awo-Affouda, A. Stollenwerk, M.B. Huang, H.G. Ramos, G. Agnello, and V.P. LaBella, *Phys. Rev. B* **71**, 033302 (2005).
2. S.A. Wolf and D.D. Awaschalom, *Science* **294,** 1488 (2001).
3. F. Priolo, G. Franzo, S. Coffa, and A. Carnera, *Phys. Rev. B* **57**, 4443 (1998).
4. J. Michel, J.L. Benton, R.F. Ferrante, D.C. Jacobson, D.J. Eaglesham, E.A. Fitzgerald, Y.H. Xie, J.M. Poate, and L.C. Kimerling, *J. Appl. Phys.* **70**, 2672 (1991).
5. J. Michel, L.V.C Assali, M.T. Morse, and L.C. Kimmerling, *Semiconductors and Semimetals* **49**, 111 (1998).
6. T.P. Das, in *Electronic Properties of Solids Using Cluster Methods*, Ed. T.A. Kaplan and S.D. Mahanti, New York and London: Plenum Press, 1995.
7. J. Andriessen, S.N. Ray, T. Lee, T.P. Das and D. Ikenberry, *Phys. Rev. A* **13**, 1669 (1976).
8. G.W. Ludwig and H.H. Woodbury, *Phys. Rev Lett.* **5**, 98 (1960).
9. H.H. Woodbury and G.W. Ludwig, *Phys. Rev* **117**, 102 (1960).
10. J.D. Carey, R.C. Barklie, J. Donegan, F. Priolo, G. Franzo, S. Coffa, *Phys. Rev. B* **59**, 2773 (1999).
11. G. Lang and W. Marshall, *Proc. Phys. Soc.* **87**, 3 (1966).
12. G. Feher, *Phys. Rev.* **114**, 1219 (1959).
13. A.G. Raffa and P. Ballone, *Phys. Rev. B* **65**, 121309 (2002).
14. T.P. Das, in *Electronic Properties of Solids Using Cluster Methods*, Ed. T.A. Kaplan and S. D. Mahanti, New York and London: Plenum Press, 1995, pp.4-6.
15. T.P. Das, *Hyperfine Interactions* **34**, 149 (1987).
16. S.D. Mahanti, T. Lee, D. Ikenberry and T.P. Das, *Phys. Rev. A* **9**, 2238 (1974).
17. Frisch, et al., *Gaussian 03, Revision C.02*, Gaussian Inc., Wallingford CT, 2004.
18. A. Abragam and B. Bleaney, *Electron Paramagnetic Resonance of Transition Ions,* Oxford: Clarendon Press, 1970.
19. J. Andriessen, S.N. Ray, T. Lee, T.P. Das and D. Ikenberry, *Phys. Rev. A* **13**, 1669 (1976), Table IX.
20. P. Raghavan, *Atomic and Nuclear Data Tables* **42**, 189 (1989).
21. J. LaRose and M.B. Huang (unpublished results).
22. M. Needels, M. Schluter, and M. Lannoo, *Phys. Rev. B* **47**, 15533 (1995).
23. M.B. Huang and X.T. Ren, *Appl. Phys. Lett.* **81**, 2734 (2002).
24. S.J. Davis, J.J. Wright, and L.C. Balling, *Phys. Rev. A* **3**, 1220 (1971).
25. J. Andriessen, K. Raghunathan, S.N. Ray, and T.P. Das, *Phys. Rev. B* **15**, 2533 (1977).
26. J. Andriessen, D. Van Ormondt, S.N. Ray, and T.P. Das, *J. Phys. B* **11**, 2601 (1978).